Article

Identification of *Trypanosoma cruzi* Growth Inhibitors with Activity In Vivo within a Collection of Licensed Drugs

Nieves Martinez-Peinado [1,†] , **Nuria Cortes-Serra** [1,†] , **Julian Sherman** [2] , **Ana Rodriguez** [2] , **Juan M. Bustamante** [3] , **Joaquim Gascon** [1] , **Maria-Jesus Pinazo** [1,*] and **Julio Alonso-Padilla** [1,*]

1   Barcelona Institute for Global Health (ISGlobal), Hospital Clínic—University of Barcelona, 08036 Barcelona, Spain; nieves.martinez@isglobal.org (N.M.-P.); nuria.cortes@isglobal.org (N.C.-S.); quim.gascon@isglobal.org (J.G.)
2   Department of Microbiology, New York University School of Medicine, New York, NY 10010, USA; Julian.Sherman@nyulangone.org (J.S.); Ana.RodriguezFernandez@nyulangone.org (A.R.)
3   Center for Tropical and Emerging Global Diseases, University of Georgia, Athens, GA 30602, USA; juanbus@uga.edu
*   Correspondence: mariajesus.pinazo@isglobal.org (M.-J.P.); julio.a.padilla@isglobal.org (J.A.-P.); Tel.: +1-0034-932275400 (ext. 1802) (M.-J.P.); +1-0034-932275400 (ext. 4569) (J.A.-P.)
†   These authors contributed equally to this work.

Abstract: Chagas disease, caused by the parasite *Trypanosoma cruzi (T. cruzi)*, affects more than six million people worldwide, with its greatest burden in Latin America. Available treatments present frequent toxicity and variable efficacy at the chronic phase of the infection, when the disease is usually diagnosed. Hence, development of new therapeutic strategies is urgent. Repositioning of licensed drugs stands as an attractive fast-track low-cost approach for the identification of safer and more effective chemotherapies. With this purpose we screened 32 licensed drugs for different indications against *T. cruzi*. We used a primary in vitro assay of Vero cells infection by *T. cruzi*. Five drugs showed potent activity rates against it ($IC_{50} < 4$ μmol L^{-1}), which were also specific (selectivity index >15) with respect to host cells. *T. cruzi* inhibitory activity of four of them was confirmed by a secondary anti-parasitic assay based on NIH-3T3 cells. Then, we assessed toxicity to human HepG2 cells and anti-amastigote specific activity of those drugs progressed. Ultimately, atovaquone-proguanil, miltefosine, and verapamil were tested in a mouse model of acute *T. cruzi* infection. Miltefosine performance in vitro and in vivo encourages further investigating its use against *T. cruzi*.

Keywords: Chagas disease; *Trypanosoma cruzi*; drugs; repositioning; phenotypic assays

1. Introduction

Chagas disease, caused by the parasite *Trypanosoma cruzi (T. cruzi)*, is a neglected disease that affects more than six million people worldwide [1]. The main burden of the infection is located in the Americas, where the disease is endemic. However, migratory movements and international travel have shifted its epidemiological profile in the last decades, and the disease is nowadays also found in non-endemic countries [1,2].

Clinically, it presents in two phases. First, there is a short acute phase (4–8 weeks long) that is usually asymptomatic and goes unnoticed and undiagnosed. Then the infection evolves to a chronic phase, in which 30% of the chronically infected subjects will develop cardiac and/or digestive symptoms that can lead to death if untreated [3].

Two drugs are currently available to treat *T. cruzi* infection: benznidazole (BNZ) and nifurtimox (NFX). Despite providing a good efficacy against the acute stage in newborns, both drugs have variable efficacy during the chronic phase of the infection [1,4]. Moreover, they require long treatment administration regimens that may lead to toxicity and frequent adverse effects, resulting in discontinuation of treatment in 20–30% of patients [5–9]. Thus, there is an urgent need to develop safer, more effective, short-course chemotherapies for reducing the burden of the disease [10].

In the last few years, several efforts have been directed towards the identification of new active compounds against *T. cruzi* [11–13]. Among those drug discovery approaches, repositioning of already licensed drugs should also be contemplated, as it stands out as an attractive fast-track and low-cost strategy [14]. Drug repositioning (also named drug repurposing or drug reprofiling) seeks finding new indications for existing drugs. Benefits of this strategy are multiple compared to the discovery and development of new chemical entities, including shortened developmental time and costs, as well as known pharmacological characteristics and safety profiles [14]. Thereby, identification of a licensed drug with potent and specific activity against *T. cruzi* could rapidly advance to clinical trials [14–16].

At present, several drug candidates have been evaluated for Chagas disease following this approach [14,16–18]. Two of the most promising, the antifungal azoles posaconazole and E1224, were identified in the context of drug repurposing [16]. They represented the first new drugs clinically evaluated for Chagas disease treatment in decades [19], which meant a breakthrough, despite the fact that they did not meet expectations and reported higher rates of therapeutic failure than BNZ in chronically infected subjects [20,21].

With the aim to identify new drugs to advance in the pipeline, in this study we have evaluated the anti-*T. cruzi* activity of 32 commercial drugs by means of state-of-the-art phenotypic assays. These guided the selection of the most active ones for their evaluation in a mouse model of acute *T. cruzi* infection, a first stage to unveil their potential to be repurposed for Chagas disease.

2. Materials and Methods

2.1. Ethical Statement

Animal studies were approved by the Institutional Animal Care and Use Committee of New York University School of Medicine (protocol #160720; approved 19 July 2019). This protocol adheres to the guidelines of the Association for Assessment and Accreditation of Laboratory Animal Care International (AAALAC).

2.2. Drugs

The collection of drugs used is shown in Table 1. Drugs presented as tablets were pulverized and dissolved in dimethyl-sulfoxide (DMSO) as 10 mmol L^{-1} stock solutions. Those already in solution were used directly in the assays at a starting concentration of 0.8 mg mL^{-1} for defibrotide, 150 mg mL^{-1} for meglumine antimoniate, 50% volume:volume (*v/v*) for beclometasone dipropionate-clioquinol, and 2.5% (*v/v*) for lidocaine. The drugs that contained two active ingredients (artemether-lumefantrine; atovaquone-proguanil; and piperaquine tetraphosphate-dyhidroartemisinin) were dissolved in DMSO by calculating its concentration based on its active ingredient: artemether, proguanil, and piperaquine tetraphosphate, respectively. A pie chart classification of the drugs used in the study per class is provided in Figure S1.

2.3. Host Cells Cultures

Vero (African green monkey kidney epithelial cells) [22], LLC-MK2 (Rhesus monkey kidney epithelial cells) [23], NIH-3T3 (Swiss albino mouse embryo fibroblast cells) [23] and HepG2 (human liver epithelial cells) [24] cultures were kept with Dulbecco´s Modified Eagle´s Medium (DMEM) supplemented with 1% penicillin-streptomycin (P-S) and 10% heat inactivated fetal bovine serum (FBS) at 37 °C, 5% CO_2 and > 95% humidity as described [23,25]. HepG2 cultures were also supplemented with 10% non-essential amino-acids.

2.4. Culture of Parasites

T. cruzi trypomastigotes from the Tulahuen strain (Discrete Typing Unit (DTU) VI) expressing β-galactosidase, or from the Brazil strain (DTU I) expressing firefly luciferase were maintained using LLC-MK2 or NIH-3T3 cells as hosts in DMEM supplemented with 2% FBS and 1% penicillin-streptomycin-glutamine (P-S-G) as described [25,55]. Between

days 5 and 7, medium containing free-swimming trypomastigotes was harvested and centrifuged for 7 min at 2500 rpm as described [12]. Trypomastigotes were allowed to swim out of the pellet for at least 3 h and used to keep the parasite cycle or for the performance of the anti-parasitic assays.

Table 1. Drugs used in the study. They are sorted by their "Trade name" in alphabetical order. (Table 1 continues in next page).

Trade Name	Active Ingredient	Class	Route of Administration	Molecular Weight (g/mol)	References
Adalat	nifedipine	calcium channel blocker	oral	346.34	[26,27]
Amlodipine Normon	amlodipine	calcium channel blocker	oral	408.88	[14,26,28]
Apocard	flecainide	antiarrhythmic	oral	414.34	[29]
Atenolol Normon	atenolol	beta blocker	oral	266.34	[14]
Biocoryl	procainamide	antiarrhythmic	oral	235.33	[14]
Bisoprolol Normon	bisoprolol	beta blocker	oral	325.44	[30]
Daraprim	pyrimethamine	antiprotozoal	oral	248.71	[14]
Defitelio	defibrotide	antithrombotic	intravenous	444.40	[31]
Diamicron	gliclazide	antidiabetic	oral	323.41	[32]
Enalapril Normon	enalapril	ACE inhibitor	oral	376.45	[14,33]
Eskazole	albendazole	antihelminthic and antiprotozoal	oral	256.33	[14]
Eurartesim	piperaquine tetraphosphate-dihydroartemisinin	antimalarial	oral	927.49–284.35	[34]
Glucantime	meglumine antimoniate	antileishmanial	intramuscular	365.98	[26,35]
Glucophage	metformin hydrochloride	antidiabetic	oral	129.16	[14]
Hemovas	pentoxifylline	hemorrheologic agent	oral	278.31	[14,36,37]
Humatin	paramomycin	antimicrobial	oral	615.63	[38]
Impavido	miltefosine	antiprotozoal	oral	407.57	[39–42]
Iver P (ELEA)	ivermectin	antihelminthic	oral	875.10	[43]
Quinine sulfate (Hospital Clinic)	quinine sulfate	antimalarial	oral	782.96	[44]
Lidocaine Braun	lidocaine	local anesthetic	intravenous	234.34	[14]
Lomper	mebendazole	antihelminthic	oral	295.29	[14]
Malarone	atovaquone-proguanil	antimalarial	oral	366.84	[45]
Manidon	verapamil	calcium channel blocker	oral/intravenous	454.60	[46–49]
Masdil	diltiazem hydrochloride	calcium channel blocker	oral	414.52	[14]
Menaderm Otológico	beclometasone dipropionate-clioquinol	fungal/antibacterial	otic	521.04–304.91	-
Nerdipina	nicardipine	calcium channel blocker	oral	479.53	[14,26]
Pentacarinat	pentamidine	antiprotozoal	intravenous/ intramuscular/ inhalation	340.42	[14,26,50,51]
Primaquine (Hospital Clinic)	primaquine	antimalarial	oral	259.35	[14,52]
Riamet	artemether-lumefrantine	antimalarial	oral	298.37–528.94	[53]
Solgol	nadolol	beta blocker	oral	309.40	[14]
Sotapor	sotalol	beta blocker	oral	272.36	[54]
Tricolam	tinidazole	antiprotozoal	oral	247.27	[14]

2.5. T. cruzi Growth Inhibition Assay

Vero cells and trypomastigotes from *T. cruzi* Tulahuen expressing β-galactosidase were harvested, centrifuged and re-suspended in DMEM without phenol red supplemented with 1% PSG, 2% FBS, 1 mmol L^{-1} sodium-pyruvate (Na-pyr) and 25 mmol L^{-1} HEPES [25]. Then, both cell types were counted and diluted at a concentration of 1×10^6 cells mL^{-1} each. Trypan blue was used to check Vero cells viability, which had to be >95% to proceed. Vero and trypomastigote cells solutions were mixed 1:1 (*v/v*) and 100 μL of that mix was added per well. That volume has 50,000 host cells and 50,000 parasites, i.e., multiplicity of infection (MOI) = 1. Test plates already contained the drugs dispensed at a starting concentration of 100 μmol L^{-1} following a 2-fold dilution pattern down to 0.05 μmol L^{-1}. BNZ was used as control of maximal drug growth inhibition in each round, while each plate contained its own negative and positive controls as described [56,57]. After four days at 37 °C, 50 μL of a PBS solution containing 0.25% NP40 and 500 μmol L^{-1} chlorophenol red-β-D-galactoside (CPRG) substrate were added per well [23]. Plates were incubated at 37 °C for 4 h and absorbance read out at 590 nm using an Epoch Gene5 spectrophotometer. All experiments were performed in triplicate.

2.6. Anti-Amastigote Specific Assay

Vero cells were seeded in T-175 flasks (5×10^6 cells per flask) in DMEM supplemented with 1% penicillin-streptomycin and 10% FBS and cultured for 24 h. Then, cells were washed once with PBS and free swimming trypomastigotes (1×10^7 trypomastigotes per flask; MOI = 1) in assay medium were added and allowed 18 h to infect [57]. After that, infected cell monolayers were washed with PBS and detached. Cells were counted and diluted to a concentration of 5×10^5 cells per mL, before adding 100 μL per well to test plates already containing the drugs dispensed as described above [57]. In all cases we included BNZ as control drug, and each plate contained its own negative (Vero cells and parasites) and positive controls (Vero cells) [57].

2.7. NIH-3T3 Cells-Based Assays

To perform the anti-parasitic assay, culture media of LLC-Mk2 cells infected with *T. cruzi* Tulahuen expressing β-galactosidase [25] was harvested, centrifuged for 7 min at $1237 \times g$ in order to eliminate the amastigotes, and trypomastigote forms were allowed to swim out of the pellet for at least 3 h at 37 °C. NIH-3T3 cells and trypomastigote solutions were mixed, and 100 μL of the mix was added per well (with 50,000 cells and 50,000 parasites each, MOI = 1) to 96-well plates already containing the drugs dispensed following a dose-response pattern at a starting concentration of 100 μmol L^{-1} in 100 μL per well (50 μmol L^{-1} final concentration in the well). Amphotericin B (Sigma-Aldrich, St. Louis, MO, USA) was used as positive control at a final concentration of 4 μmol L^{-1} [23,55]. Negative and positive controls were carried in every plate. Read out was performed as described above using a Tecan Spectra Mini plate reader.

To perform the NIH-3T3 cell toxicity assay, NIH-3T3 cells were added (50,000 cells per well) to 96-well plates already containing the drugs. After 4 days, 20 μL of Alamar Blue (Life Technologies, Eugene, OR, USA) was added. Plates were incubated for 6 h at 37 °C and fluorescence was read using a Labsystems Fluoroskan II plate reader (excitation: 544 nm, emission: 590 nm).

2.8. Vero and HepG2 Toxicity Assays

Drugs were added to culture-treated 96-well plates at a starting concentration of 800 μmol L^{-1} and 2-fold diluted for a dose-response analysis [56]. Vero and HepG2 cells were detached, centrifuged, and washed. Cell viability was checked with Trypan blue staining. Then, Vero and HepG2 cells were respectively diluted at a concentration of 5×10^5 and 3.2×10^5 cells per mL, before adding 100 μL per well. Each run contained its own negative and positive controls [56]. Plates were incubated at 37 °C for 4 days or 2 days in the case of Vero or HepG2 cells, respectively. Assays were readout by adding 50 μL per

well of a PBS solution containing 10% AlamarBlue reagent (ThermoFischer, Waltham, MA, USA) and incubating the plates for another 6 h at 37 °C before recording the fluorescence intensity in a Tecan Infinite M Nano+ reader (excitation: 530 nm, emission: 590 nm). All experiments were performed in triplicate.

2.9. T. cruzi In Vivo Inhibition Assay

Trypomastigotes from transgenic *T. cruzi* Brazil strain (DTU I) expressing firefly luciferase were purified, diluted in PBS, and injected in 8 week old female Balb/c mice (10^6 trypomastigotes per mouse). Three days after infection (day 4) mice were anesthetized by inhalation of isoflurane and injected with 150 mg per kg of D-Luciferin Potassium-salt (Goldbio, Saint Louis, MO, USA) dissolved in PBS [55]. Mice were imaged 5 to 10 min after injection of luciferin with an IVIS 100 (Xenogen, Alameda, CA, USA), and the data acquisition and analysis were performed with the software LivingImage (Xenogen, Alameda, CA, USA). On the same day 4, treatment started with oral administration of 200 μL of drugs at 30 mg per kg for atovaquone-proguanil (Malarone) and miltefosine (Impavido) [39,45], and 5 mg per kg for verapamil (Manidon) [48]. Drugs were dissolved in PBS vehicle including 0.5% hydroxymethyl cellulose and 0.4% Tween-80. The positive control group received a standard dose of 30 mg per kg of BNZ, while the negative control group received only vehicle solution [55]. Each group was formed by 5 mice. Treatment was continued daily for 10 days. On the scheduled days 4, 9 and 14, corresponding to baseline, 5 and 10 days of treatment, mice were imaged after anesthesia and injection of luciferin as described above.

2.10. Data Analysis

Absorbance and fluorescence values derived from the anti-*T. cruzi* and cell toxicity assays were normalized to the controls [12]. IC_{50} and TC_{50} values are provided as mean and standard deviation (SD). They were determined with GraphPad Prism 7 software (version 7.00, 2016) using a non-linear regression analysis model defined by Equation (1):

$$Y = 100 \div ((1 + X\char`^HillSlope) \div (IC_{50}\char`^HillSlope))$$
(1)

Total flux values recorded in the in vivo experiments are also shown as mean and SD. We used ANOVA with Bonferroni's correction for multiple comparisons to determine if the differences between groups were statistically significant.

3. Results

3.1. Anti-T. cruzi Activity on Vero Cells

T. cruzi inhibition was primarily determined by a dose-response phenotypic assay based on Vero cells infected with *T. cruzi*—Tulahuen strain (DTU VI) expressing β-galactosidase [25]. The reference drug BNZ, included as a control of drug growth inhibition in every round, had an average IC_{50} value of 1.93 (0.82) μmol L^{-1}, correlating with previous reports [25,56]. In total, we evaluated 32 drugs by the anti-*T. cruzi* phenotypic assay, wherein seven showed high anti-parasitic activity (Figure 1). Miltefosine and nifedipine were the most potent with IC_{50} values in the sub-micromolar range: 0.018 (0.0015) μmol L^{-1} and 0.19 (0.018) μmol L^{-1}, respectively (Table 2). Similarly, an IC_{50} value of 0.016 (0.0015) % (*v/v*) was reported for lidocaine (Table 2). In addition, atovaquone-proguanil and pentamidine also exhibited an anti-*T. cruzi* activity that exceeded in potency that of the reference drug BNZ, with IC_{50} values of 1.26 (0.14) μmol L^{-1} and 1.01 (0.55) μmol L^{-1}, respectively (Table 2). The other two drugs that were considered active (with IC_{50} values within 3× that of BNZ) were verapamil and piperaquine tetraphosphate - dihydroartemisinin, which showed similar IC_{50} values: 3.44 (0.44) μmol L^{-1} and 3.95 (0.51) μmol L^{-1}, respectively (Table 2). Chemical structures of these seven drugs are shown in Figure 2. IC_{50} values of the 25 drugs reported as inactive are depicted in Table S1.
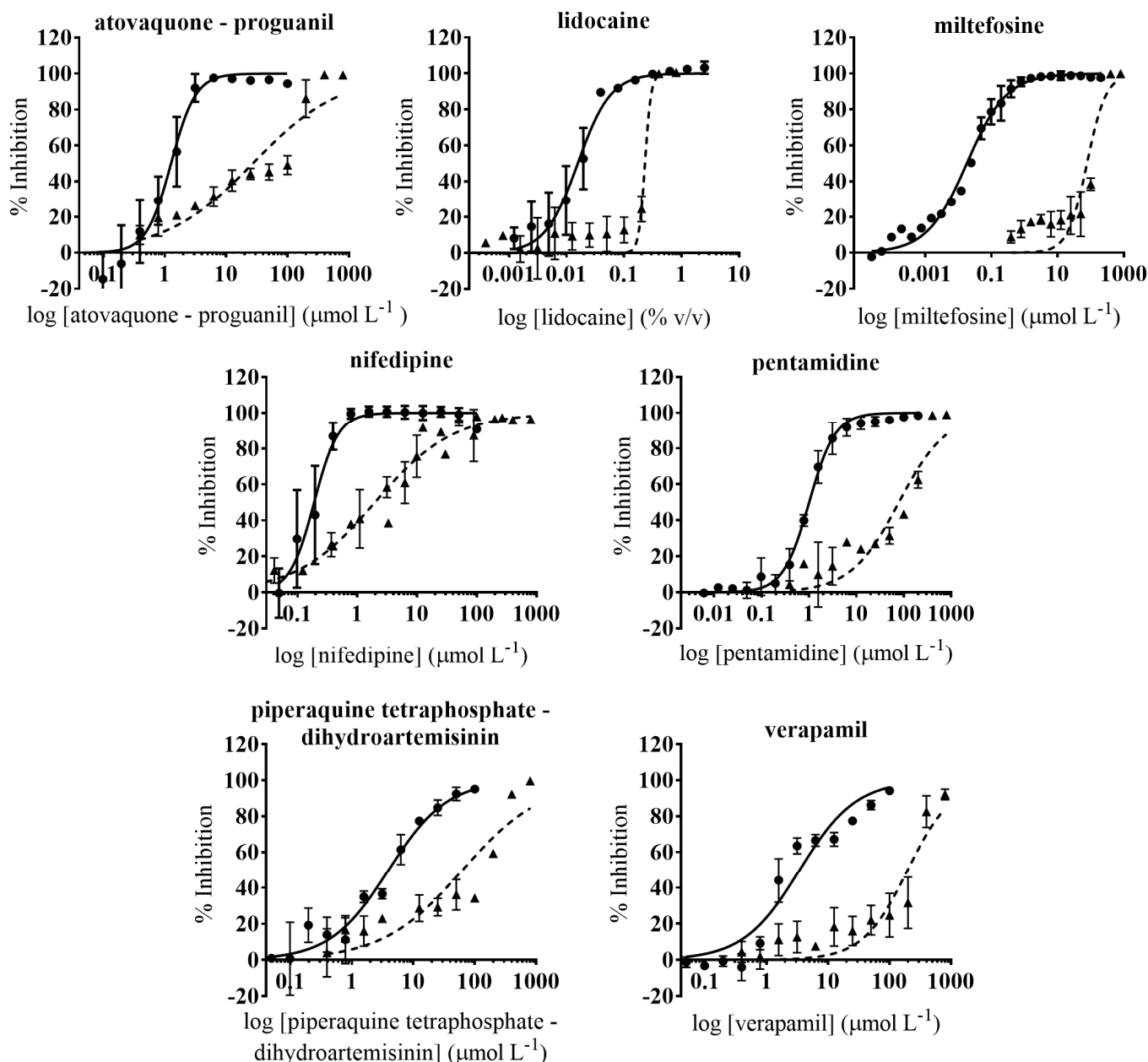
Figure 1. Dose-response curves of anti-*T. cruzi* and Vero cell toxicity assays of the seven drugs that showed an anti-parasitic activity with IC$_{50}$ values < 4 μmol L^{-1}. Anti-*T. cruzi* assay data are represented by circles and straight lines, while Vero cells toxicity data are represented by triangles and dashed lines. Graphs represent mean values and SD of at least three independent replicas.

3.2. Identification of Drugs with Specific Activity against the Parasite

Drugs that influence host cell viability would also be identified as active (false positive) in the phenotypic anti-parasitic assay. To select active ones with specific activity against *T. cruzi*, we evaluated the seven anti-parasitic active drugs in a secondary cell toxicity assay based on Vero cells [56]. In it, the reference drug BNZ had an average TC$_{50}$ value of 242.2 (13.93) μmol L^{-1} (Figure S2) in agreement with that previously reported [56,58]. Overall, the seven drugs showed low toxicity to Vero cells (Figure 1). Their TC$_{50}$/IC$_{50}$ rates or selectivity index (SI) were > 10 in all cases, a threshold that is usually considered to progress compounds with specific anti-parasitic activity [12]. Verapamil was the drug with lower toxicity to Vero cells, and registered a SI rate of 57.4 (Table 2). Similar TC$_{50}$ values were observed for miltefosine, pentamidine and piperaquine tetraphosphate-dihydroartemisinin (Table 2). Miltefosine had the widest specificity window (SI = 4388.3) (Table 2). On the other side, nifedipine and lidocaine presented SI values of 10.4 and 14.4 respectively, and their

toxicity to Vero cells was considerably higher than that retrieved for the others [nifedipine TC_{50} = 1.97 (0.27) μmol L^{-1}; lidocaine TC_{50} = 0.23 (0.027) v/v] (Table 2). Therefore, they were discarded from further progression.

Table 2. Average IC_{50}, TC_{50} and SI values of the seven primary active drugs. These were tested in phenotypic assays based on Vero, NIH-3T3 and HepG2 cells.

Drug	Vero Cells Assays			NIH-3T3 Cells Assays			HepG2 Assay	Anti-Amastigote Assay	
	[IC_{50} (SD)] μmol L^{-1}	[TC_{50} (SD)] μmol L^{-1}	SI	[IC_{50} (SD)] μmol L^{-1}	[TC_{50} (SD)] μmol L^{-1}	SI	[TC_{50} (SD)] μmol L^{-1}	[IC_{50} (SD)] μmol L^{-1}	SI
Benznidazole	1.93 (0.82)	242.2 (13.93)	125.5	-	-	-	229.8 (18.54)	2.66 (0.14)	91.1
Atovaquone-proguanil	1.26 (0.14)	27.13 (5.05)	21.5	1.32 (0.07)	>50	>50	34.36 (5.88)	1.85 (0.06)	14.7
Miltefosine	0.018 (0.0015)	78.99 (10.55)	4388.3	0.037 (0.001)	1.95 (0.57)	52.7	51.28 (7.51)	1.25 (0.05)	63.2
Lidocaine [#]	0.016 (0.0015)	0.23 (0.027)	14.4	-	-	-	-	-	-
Nifedipine	0.19 (0.018)	1.97 (0.267)	10.4	-	-	-	-	-	-
Pentamidine	1.01 (0.55)	78.96 (15.55)	78.2	0.13 (0.005)	5.9 (0.15)	45.4	39.4 (5.20)	-	-
Piperaquine tetraphosphate-dihydroartemisinin	3.95 (0.51)	75.27 (16.56)	19.1	4.05 (0.72)	27.33 (3.68)	6.8		-	-
Verapamil	3.44 (0.44)	197.4 (25.54)	57.4	0.60 (0.04)	8.16 (1.63)	13.6	170.5 (13.14)	122.5 (7.04)	1.6

[#] Lidocaine values refer to percentage of drug volume per well considering its dose-response distribution in the assay plates started at a concentration of 2.5% (v/v). SD, standard deviation; SI, selectivity index.
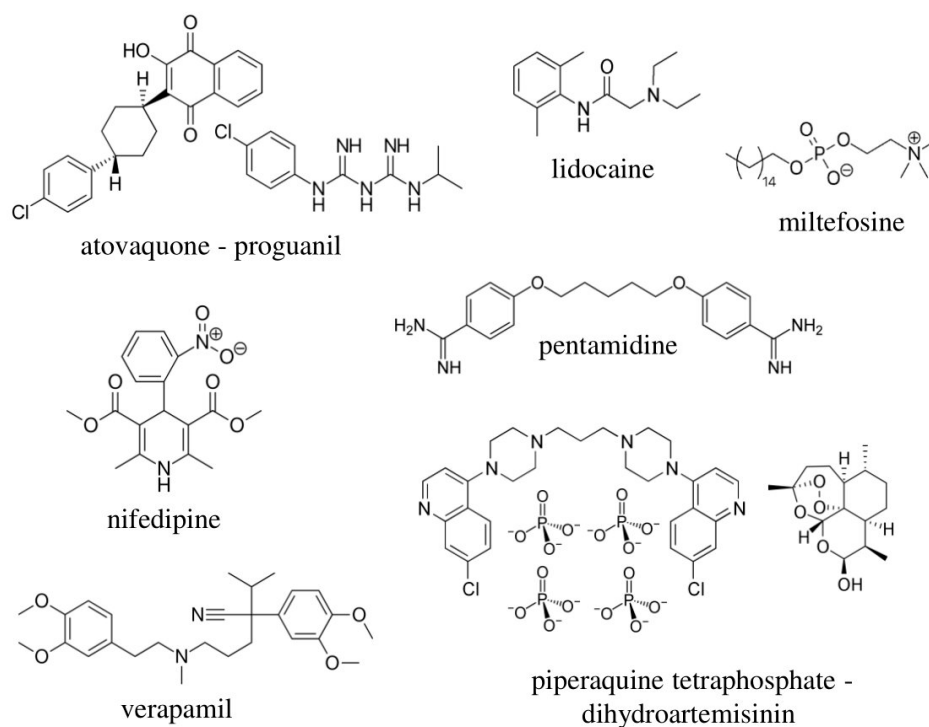

Figure 2. Chemical structures of the seven active drugs identified in the anti-parasitic assay based on Vero cells as hosts.

3.3. Anti-T. cruzi Growth Inhibition of Active Drugs Confirmed

Host cells used for the anti-*T. cruzi* assay can influence its outcome [59]. In the same manner, operational features such as the laboratory and personnel performing the assays may also bias results [60]. To address these issues we performed confirmatory assays of the five selected drugs in a different laboratory (New York University Anti-infectives Screening Core; [61]). These were based on NIH-3T3 cells as hosts and included an anti-*T. cruzi* assay and a secondary NIH-3T3 cell toxicity assay [23]. The following drugs were evaluated: atovaquone-proguanil, miltefosine, pentamidine, piperaquine tetraphosphate-dihydroartemisinin, and verapamil (Figure 3). These were selected for their specificity

(SI > 15) and anti-parasitic activity (IC_{50} < 4 µmol L^{-1}) in the assays based on Vero cells (Figure 4). To further progress the drugs, a similar anti-parasitic potency and a SI > 10 over NIH-3T3 cells were required (Figure 4).
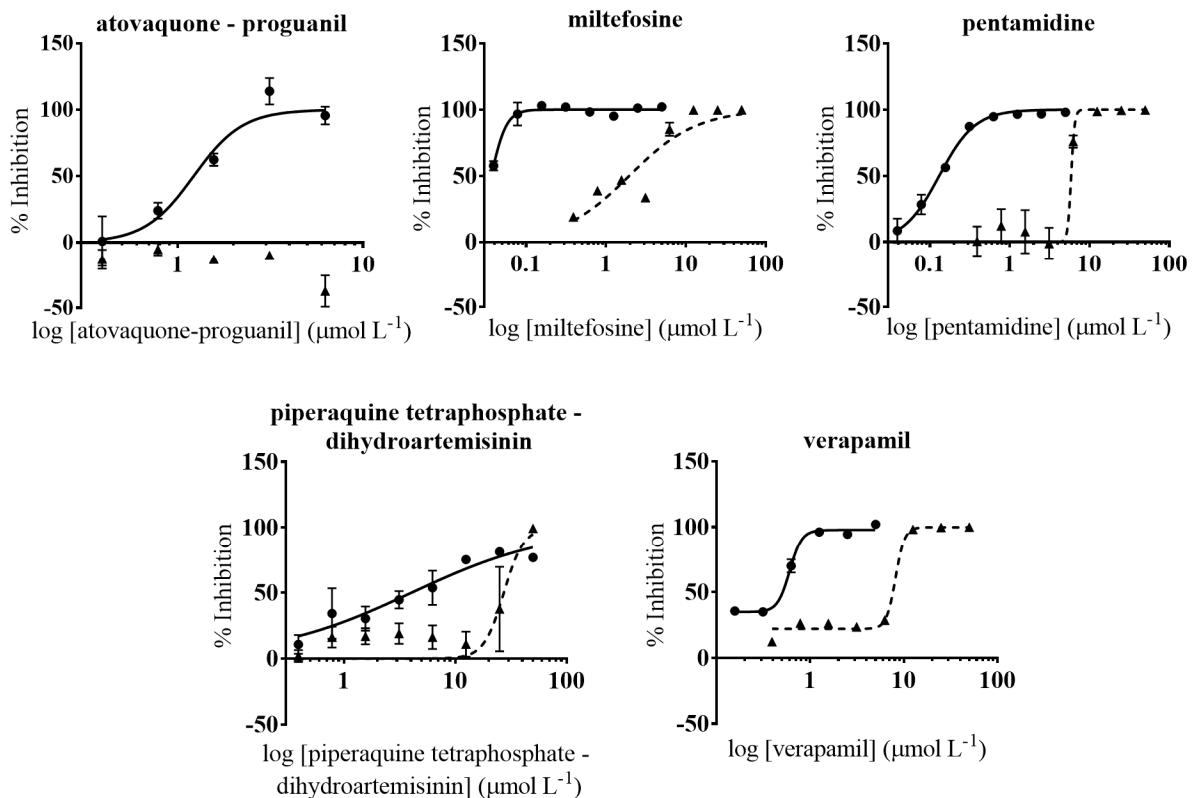

Figure 3. Dose-response curves of anti-*T. cruzi* and cell toxicity assays based on NIH-3T3 cells. Anti-*T. cruzi* assay data are represented by circles and straight lines, while NIH-3T3 cells toxicity assay data are represented by triangles and dashed lines. Graphs represent mean values and SD of at least three replicas.

Miltefosine showed similar IC_{50} values on both anti-*T. cruzi* assays: IC_{50} = 0.018 µmol L^{-1} on Vero cells, and IC_{50} = 0.037 µmol L^{-1} on NIH-3T3 cells; but it presented a considerably higher toxicity to the latter [TC_{50} = 1.95 (0.57) µmol L^{-1}] than to Vero cells [TC_{50} = 78.99 (10.55) µmol L^{-1}]. Nonetheless, in both cases its SI window prevailed > 10 and indeed was the highest amongst all the drugs evaluated (Table 2). Atovaquone-proguanil and piperaquine tetraphosphate-dihydroartemisinin exhibited a similar activity against *T. cruzi* on the assay based on Vero cells as well as on that based on NIH-3T3 (Table 2). However, the reported cytotoxicity to NIH-3T3 of the latter [TC_{50} = 27.33 (3.68) µmol L^{-1}] involved that its SI value was <10, so it was not considered parasite specific and discarded.

Anti-*T. cruzi* activity of pentamidine and verapamil in the assay based on NIH-3T3 cells was more potent than what we previously reported in the anti-*T. cruzi* assay based on Vero cells (Table 2). In terms of NIH-3T3 cells toxicity, although all three drugs also turned out to be more toxic to these than to Vero cells, their SI rates remained >10 (Table 2).

3.4. HepG2 Toxicity Assay

We next determined the toxicity over HepG2 cells of the four active drugs with confirmed activity against *T. cruzi*. Assays based on these cells are used to anticipate potential liver toxicity to human subjects [24,62]. Despite the drugs evaluated are approved for treatment of specific diseases and therefore low toxicity indexes would be expected, we included this assay in our selection cascade. BNZ and digitoxin (DTX) were used as reference drugs and their average TC_{50} values were 229.8 (18.54) µmol L^{-1} and 0.43 (0.14) µmol L^{-1}, respectively (Figure S2). All four active drugs had low toxicity to HepG2 cells, with TC_{50} values > 25 µmol L^{-1} in all cases (Figure 5, Table 2).

Similarly to what was observed in the Vero cells assay, with an average TC_{50} value of 170.5 (13.14) μmol L^{-1}, verapamil had lower toxicity to HepG2 than the other drugs (Table 2). Atovaquone-proguanil and pentamidine had similar toxicities, with TC_{50} values of 34.36 (5.88) μmol L^{-1} and 39.40 (5.20) μmol L^{-1}, respectively (Table 2).
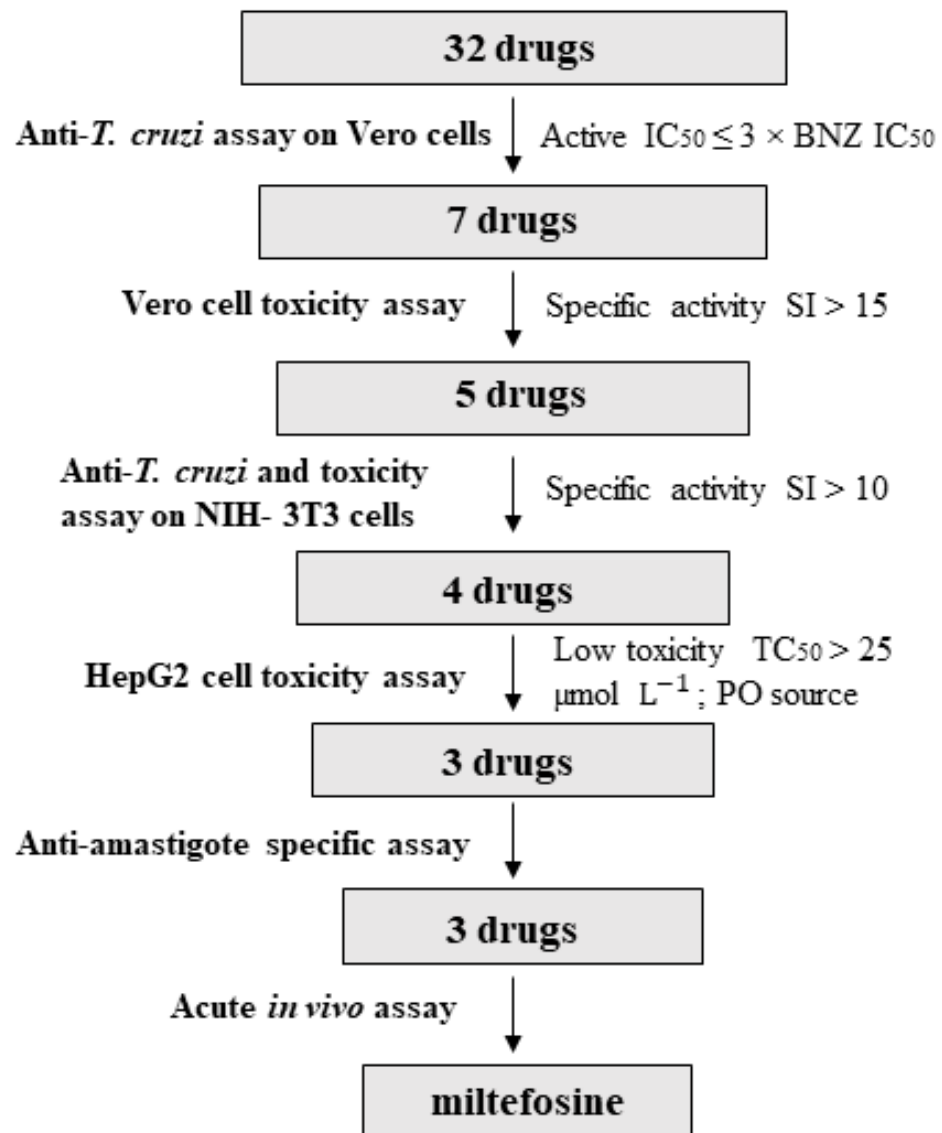

Figure 4. Flow-chart depicting the study drug progression steps (SI, selectivity index; PO, per oral source).

3.5. Anti-Amastigote Specific Activity of Selected Drugs

Amastigotes are likely the main target for any prospective anti-*T. cruzi* drug. Therefore, we progressed to anti-amastigote experiments those drugs that had been selective on the two mammalian cell lines (Vero and NIH-3T3 cells), had a $TC_{50} > 25$ μmol L^{-1} against HepG2 cells, and could be administrated orally in an in vivo model, which was the next step of the screening cascade (Figure 4). In each anti-amastigote assay we included the reference drug BNZ, registering an average IC_{50} value of 2.66 (0.14) μmol L^{-1}. Atovaquone-proguanil and miltefosine reported high anti-amastigote activity with IC_{50} values more potent than that of BNZ (Table 2, Figure 6). Moreover, both drugs reached SI values > 10 with respect to Vero cells. On the contrary, verapamil did not show specific anti-amastigote activity and had SI < 2 (Table 2, Figure 6).
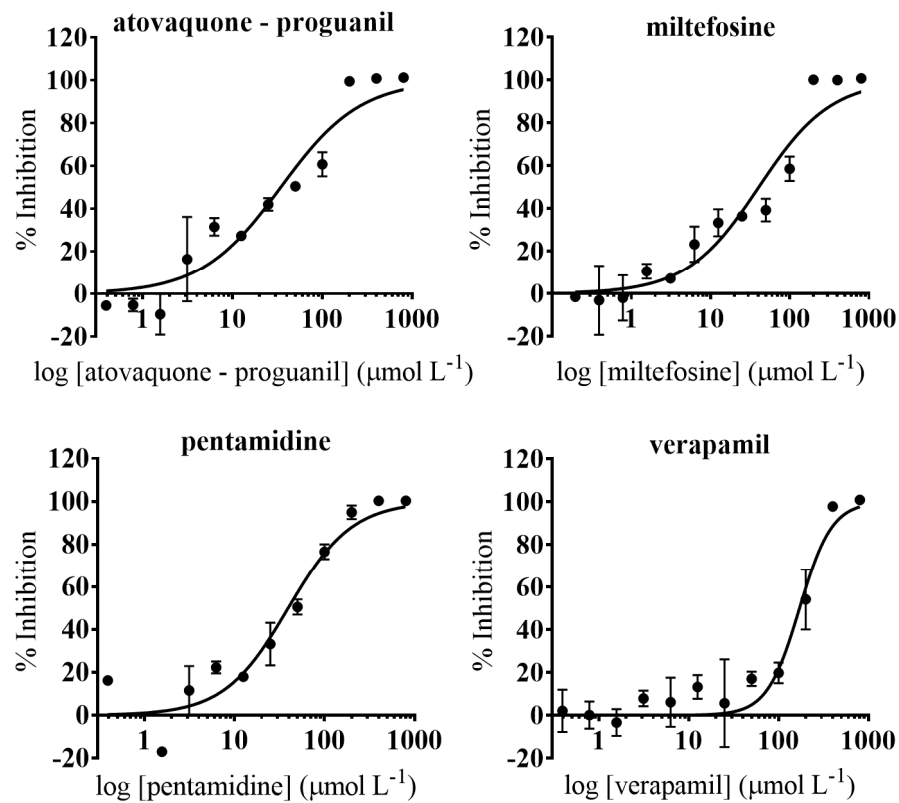
Figure 5. Dose-response curves of the four selected drugs with confirmed anti-*T. cruzi* activity assessed in HepG2 cell toxicity assays. Graphs represent mean values and SD results of at least three independent replicas.
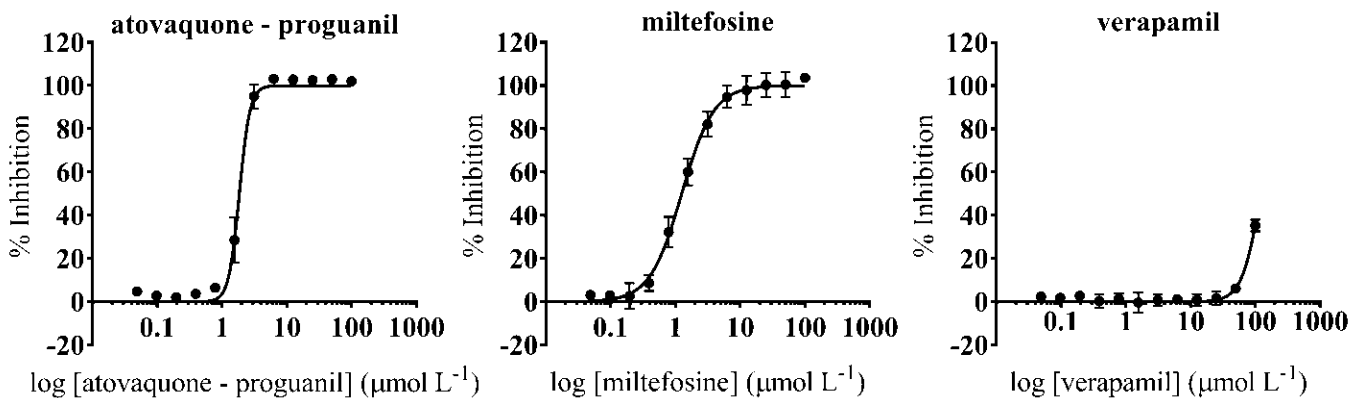

Figure 6. Dose-response curves of progressed drugs that can be orally administered in the anti-amastigote assay.

3.6. In Vivo Anti-T. cruzi Activity of the Selected Drugs in a Mouse Model of Acute Infection

We evaluated atovaquone-proguanil, miltefosine, and verapamil in vivo with an acute mouse model of *T. cruzi* infection based on transgenic parasites expressing luciferase (Figure 7) [55]. In this assay, the signal provided by luciferase in the animals is proportional to the *T. cruzi* load, and it is considered a surrogate for parasitemia [55]. One of the mice treated with miltefosine died of unknown causes after the first imaging time point (baseline). A group of animals inoculated with vehicle was included as negative control; other group of mice received a standard dose of BNZ (30 mg/kg/day) as positive control.
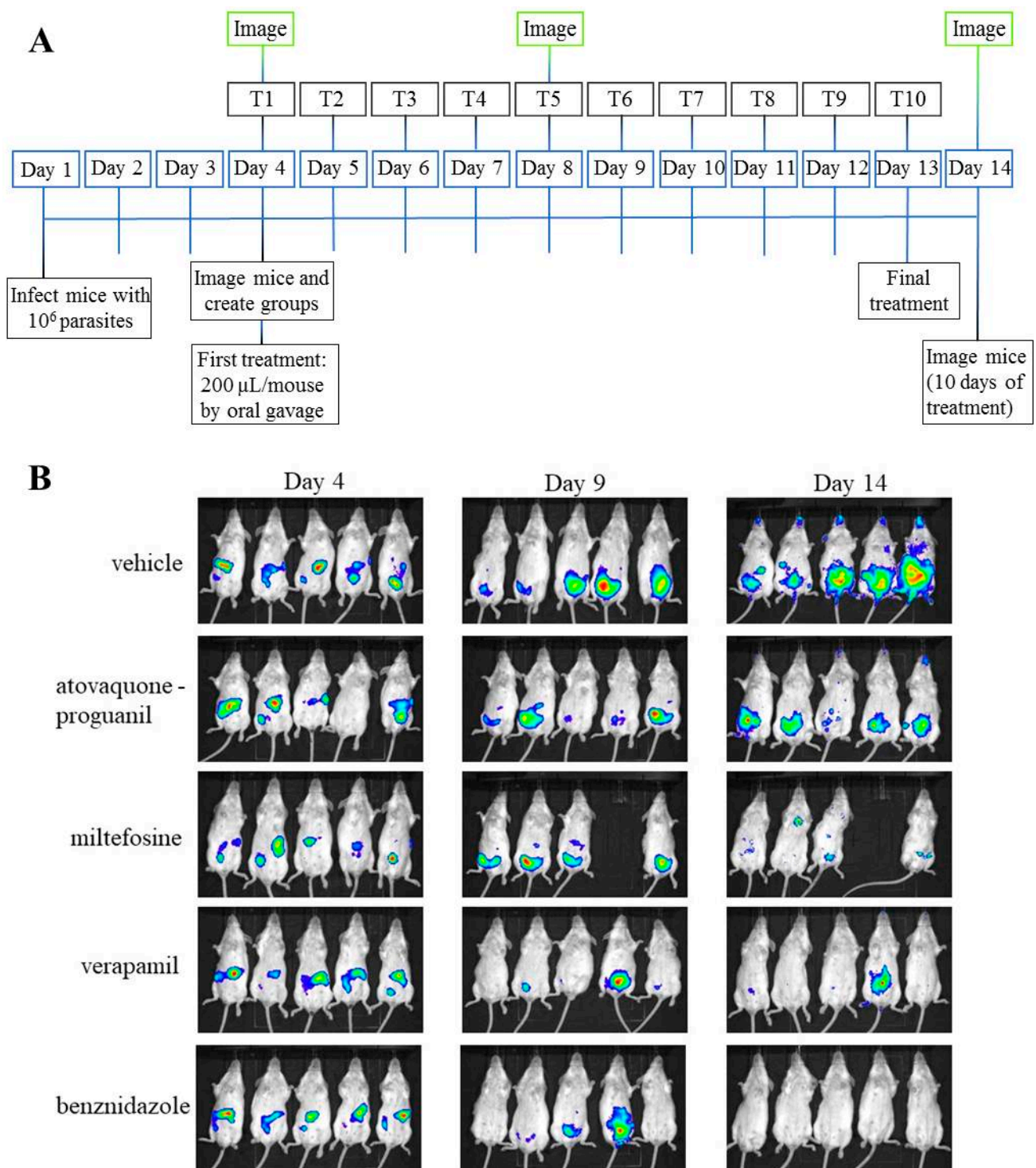
Figure 7. Scheme of the in vivo assessment of the three selected drugs against *T. cruzi* in an acute infection model (**A**) Timeline of events in the acute in vivo study (T1 to T10 depict the days of treatment). (**B**) Images of mice after 0, 5 and 10 days of treatment.

We observed that when *T. cruzi*-derived luciferase activity was registered after 5 days of treatment, only verapamil (p value = 0.038) and BNZ (p = 0.021) showed statistically significant differences versus the vehicle group (Figure 8). Such differences were also statistically significant between animals treated with atovacuone-proguanil ($p < 0.01$) and miltefosine ($p < 0.05$) compared to those treated with BNZ. In all groups except that of animals treated with atovaquone-proguanil, average *T. cruzi* parasitemia after 10 days of

treatment had significantly lower levels of parasites compared to vehicle group (Figure 8). Levels of significance of those differences were $p < 0.01$ for miltefosine- and verapamil-treated animals, and $p < 0.001$ for BNZ-treated controls. Although differences between miltefosine and verapamil groups with that of BNZ were non-significant, BNZ-treated mice outperformed the former two by $2 \times$ Log (Figure 8).
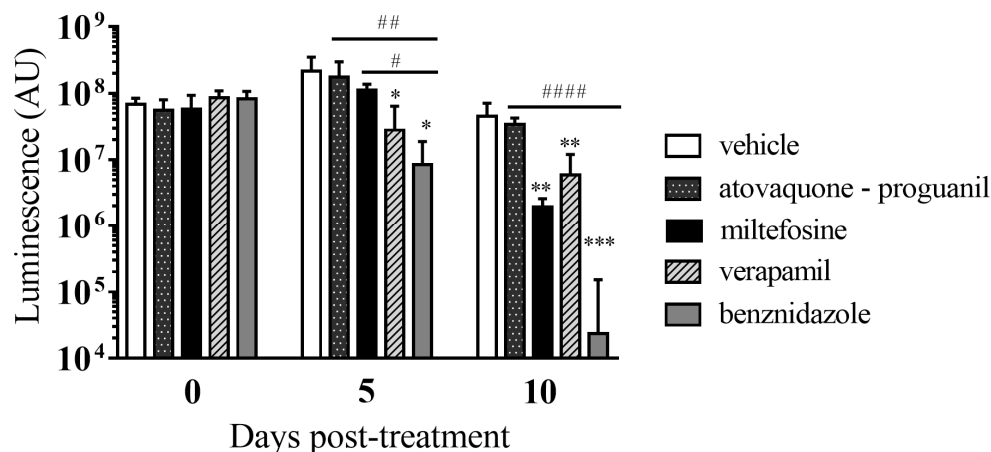

Figure 8. In vivo *T. cruzi* parasitemia (total flux) at baseline (day 0), and after 5 and 10 days of treatment. Statistically significant differences between drug-treated groups versus vehicle group or BNZ-treated group are respectively indicated by * or # symbols. One symbol indicates $p < 0.05$, two indicate $p < 0.01$, three indicate $p < 0.001$, and four symbols indicate $p < 0.0001$.

4. Discussion

Considering the long time and high costs of developing new drugs, repurposing of already licensed ones emerges as a reasonable strategy for the treatment of Neglected Tropical Diseases [14]. Recent assessment for Chagas disease of several anti-fungal azole-derivatives in clinical trials has followed that logic. With that inspiration, we selected 32 commercial drugs and tested them for their anti-*T. cruzi* activity. Seven showed high activity against the parasite, and according to the literature only four of them had been previously evaluated against *T. cruzi*: nifedipine [27], verapamil [46–49], pentamidine [50,51] and miltefosine [39–42]. After assessing host cell toxicity over Vero cells, lidocaine and nifedipine were discarded because they returned a higher toxicity rate than the rest. Anti-*T. cruzi* activity of the five remaining drugs was subject to confirmatory analysis by means of an anti-parasitic assay based on NIH-3T3 cells as hosts, which confirmed that atovaquone-proguanil, miltefosine, pentamidine, and verapamil had anti-parasitic IC_{50} values < 4 µmol L^{-1} (i.e., their IC_{50} was within $3\times$ that of BNZ), SI windows to Vero and NIH-3T3 cells were > 10, and HepG2 $TC_{50} > 25$ µmol L^{-1} [12]. Piperaquine tetraphosphate-dihydroartemisinin was toxic to NIH-3T3 and discarded from further analysis, which highlights the relevance of addressing anti-*T. cruzi* activity in more than one assay [12,59,63,64].

We further assessed the specific anti-amastigote activity of atovaquone-proguanil, miltefosine, and verapamil. Even though it was active and specific against *T. cruzi*, we discarded pentamidine given its history of severely toxic side effects upon parenteral inoculation [65,66]. Moreover, the lack of synergy between BNZ and pentamidine in an in vivo model of *T. cruzi* infection has been reported [51], and it was previously observed that it had lower activity than BNZ [50]. Thus, we decided to test in vivo the same three drugs that went to the anti-amastigote assay. Among them, miltefosine and verapamil showed statistically significant anti-parasitic activity in comparison to vehicle treated animals.

Previous studies have suggested that verapamil could have a cardio-protective effect since it was observed to ameliorate cardiac functions, mortality and morbidity in *T. cruzi* chronically infected mice [46,47]. Verapamil was the first calcium channel antagonist to be introduced into therapy in the early 1960s for the treatment of high blood pressure, heart arrhythmias, and angina [46]. To the best of our knowledge, this is the first time that verapamil is reported to have anti-*T. cruzi* activity in vitro by means of two anti-parasitic

assays based on Vero and NIH-3T3 cells. Works by Tanowitz and collaborators exploring the mechanism of action of verapamil and other calcium-channel blockers showed no inhibition of intracellular *T. cruzi* amastigotes in vitro, with which our results would correlate. However, they also reported no differences in parasitemia levels between untreated and verapamil-treated CD1 mice infected with *T. cruzi* parasites of Brazil strain, even though mortality was reduced [48,49]. Contrarily to that, we observed a statistically significant decrease of parasitemia in verapamil-treated animals in comparison to those that received vehicle, which would correlate with the anti-parasitic activity observed in the primary in vitro assay. Parasite and/or mouse strains influence the experimental outcome [59,67], and may explain to some extent the divergence of our verapamil in vivo results from those of previous studies, due to having relied on distinct mouse strains. In any case, the absence of specific anti-amastigote activity of verapamil constitutes a drawback for its progression as anti-*T. cruzi* drug.

Regarding miltefosine, although its mode of action is not fully understood, it is known to inhibit the synthesis of phosphatidylcholine in the cytosol and cytochrome-c oxidase in the mitochondria, which leads to mitochondrial dysfunction and apoptosis-like cell death [68]. A recent work by Pinto-Martinez and collaborators have provided further insight pointing at a double drug-derived action: opening of the sphingosine-activated plasma membrane Ca^{+2} channel, and direct effect on the acidocalcisome, an organelle with osmoregulatory function in *T. cruzi* [69,70]. The combine of both actions will lead to a large parasite-specific intracellular accumulation of Ca^{+2} [69]. Since disruption of the intracellular Ca^{+2} homeostasis has been described as an important drug target in trypanosomatids [40,42,71], miltefosine could indeed be an interesting drug candidate to pursue for Chagas disease. In fact, several studies have reported in vitro susceptibility of *T. cruzi* parasites to miltefosine [40–42]. For instance, Luna and coworkers reported a high susceptibility of a panel of *T. cruzi* strains against miltefosine, with an intracellular parasite growth inhibition (IC_{50}), assayed on Vero cells, that ranged between 0.082 (0.01) and 0.63 (0.13) μmol L^{-1} [40]; sub-micromolar IC_{50} values with which our results correlate. In this work, in vitro activity of miltefosine outperforms BNZ by 100× and 2× in the primary and anti-amastigote assays based on Vero cells, leading to the widest selectivity indexes calculated (Table 2).

In vivo evaluation of miltefosine was previously shown to reduce parasitemia ($<10^5$ parasites mL^{-1} in blood) in Balb/c mice infected with *T. cruzi* Y strain (DTU II) to similar levels as BNZ at day 20 post-infection [42]. Another study described a suppressive activity of miltefosine against both *T. cruzi* Y and Tulahuen strains at a dose of 30 mg per kg administered for 5 days [39]. Inspired by this study, we now provide detailed evidence of miltefosine in vivo anti-parasitic activity against a different *T. cruzi* strain (Brazil) from the widespread and pathogenic DTU I. We have used an infection model based on bioluminescent parasites that provides higher sensitivity than microscopy-based quantification of blood parasitemia.

Originally developed in the 1980s as an anti-cancer agent, miltefosine is the only oral treatment approved for leishmaniasis [68,72]. Its registration to treat fatal visceral leishmaniasis was considered a breakthrough, but some limitations have been observed thereafter, including frequent side effects driving treatment discontinuation and failure, appearance of resistances, and low availability and affordability [68,73]. These features might discourage its use for Chagas disease. However, given the very good results we have observed in vitro, particularly the very wide SI, and its inhibitory capacity in an acute in vivo infection, it is worth the further assessment of miltefosine's performance in a chronic model of *T. cruzi* infection. Similarly, it remains to be elucidated whether its co-administration with BNZ would serve to reduce the dosage of the latter without compromising its efficacy, with the aim of limiting side effects.

5. Conclusions

Despite the recent failure of azole-derivatives in clinical trials, drug repurposing is still the fastest and cheapest strategy to identify new treatments for Chagas disease. Out of the 32 drugs for different indications evaluated in this study, we found that miltefosine and verapamil reduced parasitemia in a mouse model of acute *T. cruzi* infection after ten days of treatment with 30 and 5 mg per kg, respectively, expanding previously obtained results by others. Although a similar dose of BNZ had a higher inhibitory effect, taking into consideration that miltefosine was shown to specifically inhibit the parasite intracellular replicative stage, and its indication for the oral treatment of leishmaniasis, its potential use against *T. cruzi* should be further investigated. Moreover, miltefosine had the widest activity windows, which may allow testing it at higher doses or under alternative regimes, including its co-administration with BNZ.

References

1. WHO: Chagas Disease (American Trypanosomiasis). Available online: https://www.who.int/en/news-room/fact-sheets/detail/chagas-disease-(american-trypanosomiasis) (accessed on 26 January 2020).
2. Gascon, J.; Bern, C.; Pinazo, M.J. Chagas disease in Spain, the United States and other non-endemic countries. *Acta Trop.* **2010**, *115*, 22–27. [CrossRef]
3. Pérez-Molina, J.A.; Molina, I. Chagas disease. *Lancet* **2018**, *391*, 82–94. [CrossRef]
4. Fabbro, D.L.; Streiger, M.L.; Arias, E.D.; Bizai, M.L.; Del Barco, M.; Amicone, N.A. Trypanocide treatment among adults with chronic Chagas disease living in Santa Fe City (Argentina), over a mean follow-up of 21 years: Parasitological, serological and clinical evolution. *Rev. Soc. Bras. Med. Trop.* **2007**, *40*, 1–10. [CrossRef]

5. Alonso-Padilla, J.; Cortés-Serra, N.; Pinazo, M.J.; Elena, M.; Abril, M.; Barreira, F.; Sosa-Estani, S.; Hotez, P.J.; Gascón, J. Strategies to enhance access to diagnosis and treatment for Chagas disease patients in Latin America. *Expert Rev. Anti. Infect. Ther.* **2019**, *17*, 145–157. [CrossRef]

6. Crespillo, C.; Emmanuele, A.; Rullo, V.; López, R.; Begoña, V.; Maillo, M. Safety profile of benznidazole in the treatment of chronic Chagas disease: Experience of a referral centre and systematic literature review with meta-analysis. *Drug Saf.* **2018**, *41*, 1035–1048. [CrossRef]

7. Forsyth, C.J.; Hernandez, S.; Olmedo, W.; Abuhamidah, A.; Traina, M.I.; Sanchez, D.R.; Soverow, J.; Meymandi, S.K. Safety profile of nifurtimox for treatment of Chagas disease in the United States. *Clin. Infect. Dis.* **2016**, *63*, 1056–1062. [CrossRef]

8. Pinazo, M.J.; Muñoz, J.; Posada, E.; López-Chejade, P.; Gállego, M.; Ayala, E.; Del Cacho, E.; Soy, D.; Gascon, J. Tolerance of benznidazole in treatment of Chagas' disease in adults. *Antimicrob. Agents Chemother.* **2010**, *54*, 4896–4899. [CrossRef]

9. Jackson, Y.; Alirol, E.; Getaz, L.; Wolff, H.; Combescure, C.; Chappuis, F. Tolerance and safety of nifurtimox in patients with chronic Chagas disease. *Clin. Infect. Dis.* **2010**, *51*, e69–e75. [CrossRef]

10. Urbina, J.A. New insights in Chagas' disease treatment. *Drugs Future* **2010**, *35*, 409–419. [CrossRef]

11. Khare, S.; Nagle, A.S.; Biggart, A.; Lai, Y.H.; Liang, F.; Davis, L.C.; Barnes, S.W.; Mathison, C.J.N.; Myburgh, E.; Gao, M.Y.; et al. Proteasome inhibition for treatment of leishmaniasis, Chagas disease and sleeping sickness. *Nature* **2016**, *537*, 229–233. [CrossRef]

12. Peña, I.; Pilar Manzano, M.; Cantizani, J.; Kessler, A.; Alonso-Padilla, J.; Bardera, A.I.; Alvarez, E.; Colmenarejo, G.; Cotillo, I.; Roquero, I.; et al. New compound sets identified from high throughput phenotypic screening against three kinetoplastid parasites: An open resource. *Sci. Rep.* **2015**, *5*, 8771.

13. Martínez-Peinado, N.; Cortes-Serra, N.; Losada-Galvan, I.; Alonso-Vega, C.; Urbina, J.A.; Rodríguez, A.; VandeBerg, J.L.; Pinazo, M.J.; Gascon, J.; Alonso-Padilla, J. Emerging agents for the treatment of Chagas disease: What is in the preclinical and clinical development pipeline? *Expert Opin. Investig. Drugs* **2020**, *9*, 947–959. [CrossRef]

14. Planer, J.D.; Hulverson, M.A.; Arif, J.A.; Ranade, R.M.; Don, R.; Buckner, F.S. Synergy testing of FDA-approved drugs identifies potent drug combinations against *Trypanosoma cruzi*. *PLoS Negl. Trop. Dis.* **2014**, *8*, e2977. [CrossRef] [PubMed]

15. Berenstein, A.J.; Magariños, M.P.; Chernomoretz, A.; Agüero, F. A multilayer network approach for guiding drug repositioning in neglected diseases. *PLoS Negl. Trop. Dis.* **2016**, *10*, 1–33. [CrossRef]

16. Simões-Silva, M.R.; De Araújo, J.S.; Oliveira, G.M.; Demarque, K.C.; Peres, R.B.; D'Almeida-Melo, I.; Batista, D.G.J.; Da Silva, C.F.; Cardoso-Santos, C.; Da Silva, P.B.; et al. Drug repurposing strategy against *Trypanosoma cruzi* infection: In vitro and in vivo assessment of the activity of metronidazole in mono- and combined therapy. *Biochem. Pharmacol.* **2017**, *145*, 46–53.

17. Ferreira, D.D.; Mesquita, J.T.; Da Costa Silva, T.A.; Romanelli, M.M.; Da Gama Jaen Batista, D.; Da Silva, C.F.; Da Gama, A.N.S.; Neves, B.J.; Melo-Filho, C.C.; Correia Soeiro, M.D.N.; et al. Efficacy of sertraline against *Trypanosoma cruzi*: An in vitro and in silico study. *J. Venom. Anim. Toxins Incl. Trop. Dis.* **2018**, *24*, 30. [CrossRef]

18. Kaiser, M.; Mäser, P.; Tadoori, L.P.; Ioset, J.R.; Brun, R.; Sullivan, D.J. Antiprotozoal activity profiling of approved drugs: A starting point toward drug repositioning. *PLoS One* **2015**, *10*, e0135556. [CrossRef]

19. Alonso-Vega, C.; Losada-Galván, I.; Pinazo, M.J.; Sancho Mas, J.; Brustenga, J.G.; Alonso-Padilla, J. The senseless orphanage of Chagas Disease. *Expert Opin. Orphan Drugs* **2019**, *7*, 535–545. [CrossRef]

20. Molina, I.; Goḿez I Prat, J.; Salvador, F.; Treviño, B.; Sulleiro, E.; Serre, N.; Pou, D.; Roure, S.; Cabezos, J.; Valerio, L.; et al. Randomized trial of posaconazole and benznidazole for chronic Chagas' disease. *N. Engl. J. Med.* **2014**, *370*, 1899–1908. [CrossRef]

21. Torrico, F.; Gascon, J.; Ortiz, L.; Alonso-Vega, C.; Pinazo, M.J.; Schijman, A.; Almeida, I.C.; Alves, F.; Strub-Wourgaft, N.; Ribeiro, I.; et al. Treatment of adult chronic indeterminate Chagas disease with benznidazole and three E1224 dosing regimens: A proof-of-concept, randomised, placebo-controlled trial. *Lancet Infect. Dis.* **2018**, *18*, 419–430. [CrossRef]

22. Mosca, J.D.; Pitha, P.M. Transcriptional and posttranscriptional regulation of exogenous human beta interferon gene in simian cells defective in interferon synthesis. *Mol. Cell. Biol.* **1986**, *6*, 2279–2283. [CrossRef]

23. Bettiol, E.; Samanovic, M.; Murkin, A.S.; Raper, J.; Buckner, F.; Rodriguez, A. Identification of three classes of heteroaromatic compounds with activity against intracellular *Trypanosoma cruzi* by chemical library screening. *PLoS Negl. Trop. Dis.* **2009**, *3*, e384. [CrossRef] [PubMed]

24. Choi, J.M.; Oh, S.J.; Lee, S.Y.; Im, J.H.; Oh, J.M.; Ryu, C.S.; Kwak, H.C.; Lee, J.Y.; Kang, K.W.; Kim, S.K. HepG2 cells as an in vitro model for evaluation of cytochrome P450 induction by xenobiotics. *Arch. Pharm. Res.* **2015**, *38*, 691–704. [CrossRef] [PubMed]

25. Buckner, F.S.; Verlinde, C.L.M.J.; La Flamme, A.C.; Van Voorhis, W.C. Efficient technique for screening drugs for activity against *Trypanosoma cruzi* using parasites expressing β-Galactosidase. *Antimicrob. Agents Chemother.* **1996**, *40*, 2592–2597. [CrossRef] [PubMed]

26. Reimão, J.Q.; Scotti, M.T.; Tempone, A.G. Anti-leishmanial and anti-trypanosomal activities of 1,4-dihydropyridines: In vitro evaluation and structure-activity relationship study. *Bioorganic Med. Chem.* **2010**, *18*, 8044–8053. [CrossRef]

27. Borges Migliavaca, C.; Stein, C.; Colpani, V.; René Pinto de Sousa Miguel, S.; Nascimento Cruz, L.; Oliveira Dantas, R.; Falavigna, M. Isosorbide and nifedipine for Chagas' megaesophagus: A systematic review and meta-analysis. *PLoS Negl. Trop. Dis.* **2018**, *12*, 1–13. [CrossRef]

28. De Rycker, M.; Thomas, J.; Riley, J.; Brough, S.J.; Miles, T.J.; Gray, D.W. Identification of trypanocidal activity for known clinical compounds using a new *Trypanosoma cruzi* hit-discovery screening cascade. *PLoS Negl. Trop. Dis.* **2016**, *10*, e0004584. [CrossRef]

29. Paolini, E.; Stronati, G.; Guerra, F.; Capucci, A. Flecainide: Electrophysiological properties, clinical indications, and practical aspects. *Pharmacol. Res.* **2019**, *148*, 10443.

30. Quiros, F.R.; Morillo, C.A.; Casas, J.P.; Cubillos, L.A.; Silva, F.A. Charity: Chagas cardiomyopathy bisoprolol intervention study: A randomized double-blind placebo force-titration controlled study with bisoprolol in patients with chronic heart failure secondary to Chagas cardiomyopathy [NCT00323973]. *Trials* **2006**, *7*, 21. [CrossRef]

31. Stein, C.; Castanotto, D.; Krishnan, A.; Nikolaenko, L. Defibrotide (Defitelio): A new addition to the stockpile of food and drug administration-approved oligonucleotide drugs. *Molecular Therapy - Nucleic Acids.* **2016**, *5*, e346. [CrossRef]

32. Landman, G.W.D.; De Bock, G.H.; Van Hateren, K.J.J.; Van Dijk, P.R.; Groenier, K.H.; Gans, R.O.B.; Houweling, S.T.; Bilo, H.J.G.; Kleefstra, N. Safety and efficacy of gliclazide as treatment for type 2 diabetes: A systematic review and meta-analysis of randomized Trials. *PLoS One* **2014**, *9*, e82880. [CrossRef]

33. Penitente, A.R.; Leite, A.L.J.; Costa, G.D.P.; Shrestha, D.; Horta, A.L.; Natali, A.J.; Neves, C.A.; Talvani, A. Enalapril in combination with benznidazole reduces cardiac inflammation and creatine kinases in mice chronically infected with *Trypanosoma cruzi*. *Am. J. Trop. Med. Hyg.* **2015**, *93*, 976–982. [CrossRef]

34. Loo, C.S.N.; Lam, N.S.K.; Yu, D.; Su, X.Z.; Lu, F. Artemisinin and its derivatives in treating protozoan infections beyond malaria. *Pharmacol. Res.* **2017**, *117*, 192–217. [CrossRef]

35. Moreira, V.R.; De Jesus, L.C.L.; Soares, R.E.P.; Silva, L.D.M.; Pinto, B.A.S.; Melo, M.N.; De AndradePaes, A.M.; Pereira, S.R.F. Meglumine antimoniate (Glucantime) causes oxidative stress-derived DNA damage in Balb/c mice infected by *Leishmania* (Leishmania) *infantum*. *Antimicrob. Agents Chemother.* **2017**, *61*, e02360-16. [CrossRef]

36. Andrade, S.G.; Magalhães, L.D.A.; Pessina, D.H. Importance of TNF-α in the course of acute infection with *Trypanosoma cruzi*: Influence of its inhibition by pentoxifylline treatment. *Mem. Inst. Oswaldo Cruz* **2008**, *103*, 21–26. [CrossRef] [PubMed]

37. Pereira, I.R.; Vilar-Pereira, G.; Moreira, O.C.; Ramos, I.P.; Gibaldi, D.; Britto, C.; Moraes, M.O.; Lannes-Vieira, J. Pentoxifylline reverses chronic experimental chagasic cardiomyopathy in association with repositioning of abnormal CD8+ T-cell response. *PLoS Negl. Trop. Dis.* **2015**, *9*, e0003659.

38. Hobbie, S.N.; Kaiser, M.; Schmidt, S.; Shcherbakov, D.; Janusic, T.; Brun, R.; Böttger, E.C. Genetic reconstruction of protozoan RRNA decoding sites provides a rationale for paromomycin activity against *Leishmania* and *Trypanosoma*. *PLoS Negl. Trop. Dis.* **2011**, *5*, e1161. [CrossRef] [PubMed]

39. Croft, S.L.; Snowdon, D.; Yardley, V. The activities of four anticancer alkyllysophospholipids against *Leishmania donovani*, *Trypanosoma cruzi* and *Trypanosoma brucei*. *J. Antimicrob. Chemother.* **1996**, *38*, 1041–1047. [CrossRef]

40. Luna, K.P.; Hernandez, I.P.; Rueda, C.M.; Zorro, M.M.; Croft, S.L.; Escobar, P. In vitro susceptibility of *Trypanosoma cruzi* strains from Santander, Colombia, to hexadecylphosphocholine (Miltefosine), nifurtimox and benznidazole. *Biomedica* **2009**, *29*, 448–455.

41. Santa-Rita, R.M.; Santos Barbosa, H.; Meirelles, M.D.N.S.L.; De Castro, S.L. Effect of the alkyl-lysophospholipids on the proliferation and differentiation of *Trypanosoma cruzi*. *Acta Trop.* **2000**, *75*, 219–228.

42. Saraiva, V.B.; Gibaldi, D.; Previato, J.O.; Mendonça-Previato, L.; Bozza, M.T.; Freire-de-Lima, C.G.; Heise, N. Proinflammatory and cytotoxic effects of hexadecylphosphocholine (miltefosine) against drug-resistant strains of *Trypanosoma cruzi*. *Antimicrob. Agents Chemother.* **2002**, *46*, 3472–3477. [CrossRef]

43. Dias, J.C.P.; Schofield, C.J.; Machado, E.M.M.; Fernandes, A.J. Ticks, ivermectin, and experimental Chagas disease. *Mem. Inst. Oswaldo Cruz* **2005**, *100*, 829–832. [CrossRef]

44. Achan, J.; Talisuna, A.O.; Erhart, A.; Yeka, A.; Tibenderana, J.K.; Baliraine, F.N.; Rosenthal, P.J.; D'Alessandro, U. Quinine, an old anti-malarial drug in a modern world: Role in the treatment of malaria. *Malar. J.* **2011**, *10*, 144. [CrossRef]

45. Flannery, E.L.; Foquet, L.; Chuenchob, V.; Fishbaugher, M.; Billman, Z.; Navarro, M.J.; Betz, W.; Olsen, T.M.; Lee, J.; Camargo, N.; et al. Assessing drug efficacy against *Plasmodium falciparum* liver stages in vivo. *JCI Insight* **2018**, *3*, e92587. [CrossRef] [PubMed]

46. Morris, S.A.; Weiss, L.M.; Factor, S.; Bilezikian, J.P.; Tanowitz, H.; Wittner, M. Verapamil ameliorates clinical, pathologic and biochemical manifestations of experimental chagasic cardiomyopathy in mice. *J. Am. Coll. Cardiol.* **1989**, *14*, 782–789. [CrossRef]

47. Tanowitz, H.B.; Morris, S.A.; Weiss, L.M.; Bilezikian, J.P.; Factor, S.M.; Wittner, M. Effect of verapamil on the development of chronic experimental Chagas' disease. *Am. J. Trop. Med. Hyg.* **1989**, *41*, 643–649. [CrossRef]

48. Tanowitz, H.B.; Wittner, M.; Chen, B.; Huang, H.; Weiss, L.M.; Christ, G.J.; Braunstein, V.; Bilezikian, J.P.; Morris, S.A. Effects of verapamil on acute murine Chagas' disease. *J. Parasitol.* **1996**, *82*, 814. [CrossRef] [PubMed]

49. De Souza, A.P.; Tanowitz, H.B.; Chandra, M.; Shtutin, V.; Weiss, L.M.; Morris, S.A.; Factor, S.M.; Huang, H.; Wittner, M.; Shirani, J.; et al. Effects of early and late verapamil administration on the development of cardiomyopathy in experimental chronic *Trypanosoma cruzi* (Brazil Strain) infection. *Parasitol. Res.* **2004**, *92*, 496–501.

50. Díaz, M.V.; Miranda, M.R.; Campos-Estrada, C.; Reigada, C.; Maya, J.D.; Pereira, C.A.; López-Muñoz, R. Pentamidine exerts in vitro and in vivo anti *Trypanosoma cruzi* activity and inhibits the polyamine transport in *Trypanosoma cruzi*. *Acta Trop.* **2014**, *134*, 1–9. [CrossRef]

51. Seguel, V.; Castro, L.; Reigada, C.; Cortes, L.; Díaz, M.V.; Miranda, M.R.; Pereira, C.A.; Lapier, M.; Campos-Estrada, C.; Morello, A.; et al. Pentamidine antagonizes the benznidazole's effect in vitro, and lacks of synergy in vivo: Implications about the polyamine transport as an anti-*Trypanosoma cruzi* target. *Exp. Parasitol.* **2016**, *171*, 23–32. [CrossRef] [PubMed]

52. McCabe, R. Primaquine is lethal for intracellular but not extracellular *Trypanosoma cruzi*. *J. Parasitol.* **1988**, *74*, 748–753. [CrossRef]

53. van der Pluijm, R.W.; Tripura, R.; Hoglund, R.M.; Pyae Phyo, A.; Lek, D.; ul Islam, A.; Anvikar, A.R.; Satpathi, P.; Satpathi, S.; Behera, P.K.; et al. Triple artemisinin-based combination therapies versus artemisinin-based combination therapies for uncomplicated *Plasmodium falciparum* malaria: A multicentre, open-label, randomised clinical trial. *Lancet* **2020**, *395*, 1345–1360. [CrossRef]

54. Leite, L.R.; Fenelon, G.; Simoes, A.; Silva, G.G.; Friedman, P.A.; De Paola, A.A.V. Clinical usefulness of electrophysiologic testing in patients with ventricular tachycardia and chronic chagasic cardiomyopathy treated with amiodarone or sotalol. *J. Cardiovasc. Electrophysiol.* **2003**, *14*, 567–573.

55. Andriani, G.; Chessler, A.-D.C.; Courtemanche, G.; Burleigh, B.A.; Rodriguez, A. Activity in vivo of anti-*Trypanosoma cruzi* compounds selected from a high throughput screening. *PLoS Negl. Trop. Dis.* **2011**, *5*, e1298. [CrossRef]

56. Martinez-Peinado, N.; Cortes-Serra, N.; Torras-Claveria, L.; Pinazo, M.-J.; Gascon, J.; Bastida, J.; Alonso-Padilla, J. Amaryllidaceae alkaloids with anti-*Trypanosoma cruzi* activity. *Parasit. Vectors* **2020**, *13*, 299. [PubMed]

57. Martinez-Peinado, N.; Martori, C.; Cortes-Serra, N.; Sherman, J.; Rodriguez, A.; Gascon, J.; Alberola, J.; Pinazo, M.-J.; Rodriguez-Cortes, A.; Alonso-Padilla, J. Anti-*Trypanosoma cruzi* activity of metabolism modifier compounds. *Int. J. Mol. Sci.* **2021**, *22*, 688. [CrossRef]

58. Alonso-Padilla, J.; Cotillo, I.; Presa, J.L.; Cantizani, J.; Peña, I.; Bardera, A.I.; Martín, J.J.; Rodriguez, A. Automated high-content assay for compounds selectively toxic to *Trypanosoma cruzi* in a myoblastic cell line. *PLoS Negl. Trop. Dis.* **2015**, *9*, e0003493. [CrossRef]

59. Franco, C.H.; Alcântara, L.M.; Chatelain, E.; Freitas-Junior, L.; Moraes, C.B. Drug discovery for Chagas disease: Impact of different host cell lines on assay performance and hit compound selection. *Trop. Med. Infect. Dis.* **2019**, *4*, 82.

60. Mitchel, F.L. The implementation of quality control and factors affecting its success. *Ann. Clin. Biochem.* **1969**, *6*, 119–122. [CrossRef]

61. Anti-Infectives Screening Core Services | NYU Langone Health. Available online: https://med.nyu.edu/research/scientific-cores-shared-resources/anti-infectives-screening-core/services (accessed on 28 January 2021).

62. Crouch, S.P.M.; Kozlowski, R.; Slater, K.J.; Fletcher, J. The use of ATP bioluminescence as a measure of cell proliferation and cytotoxicity. *J. Immunol. Methods* **1993**, *160*, 81–88.

63. Francisco, A.F.; Jayawardhana, S.; Lewis, M.D.; Taylor, M.C.; Kelly, J.M. Biological factors that impinge on Chagas disease drug development. *Parasitology* **2017**, *144*, 1871–1880. [CrossRef]

64. Lewis, M.D.; Francisco, A.F.; Taylor, M.C.; Kelly, J.M. A new experimental model for assessing drug efficacy against *Trypanosoma cruzi* infection based on highly sensitive in vivo imaging. *J. Biomol. Screen.* **2015**, *20*, 36–43.

65. Timm, B.L.; Da Silva, P.B.; Batista, M.M.; Farahat, A.A.; Kumar, A.; Boykin, D.W.; Soeiro, M.N.C. In vitro investigation of the efficacy of novel diamidines against Trypanosoma cruzi. *Parasitology* **2014**, *141*, 1272–1276. [CrossRef]

66. Wispelwey, B.; Pearson, R. Pentamidine: A risk-benefit analysis. *Drug Saf.* **1990**, *5*, 212–219. [CrossRef]

67. Lewis, M.D.; Francisco, A.F.; Taylor, M.C.; Jayawardhana, S.; Kelly, J.M. Host and parasite genetics shape a link between *Trypanosoma cruzi* infection dynamics and chronic cardiomyopathy. *Cell Microbiol.* **2016**, *18*, 1429–1443. [CrossRef]

68. Sunyoto, T.; Potet, J.; Boelaert, M. Why miltefosine—A life-saving drug for leishmaniasis—Is unavailable to people who need it the most. *BMJ Glob. Health* **2018**, *3*, e000709. [CrossRef] [PubMed]

69. Pinto-Martinez, A.K.; Rodriguez-Durán, J.; Serrano-Martin, X.; Hernandez-Rodriguez, V.; Benaim, G. Mechanism of action of miltefosine on *Leishmania donovani* involves the impairment of acidocalcisome function and the activation of the sphingosine-dependent plasma membrane Ca^{2+} channel. *Antimicrob. Agents Chemother.* **2018**, *62*, e01614-17. [CrossRef]

70. Rohloff, P.; Montalvetti, A.; Docampo, R. Acidocalcisomes and the contractile vacuole complex are involved in osmoregulation in *Trypanosoma cruzi*. *J. Biol. Chem.* **2004**, *279*, 52270–52281.

71. Benaim, G.; Paniz-Mondolfi, A.E.; Sordillo, E.M.; Martinez-Sotillo, N. Disruption of intracellular calcium homeostasis as a therapeutic target against *Trypanosoma cruzi*. *Front. Cell. Infect. Microbiol.* **2020**, *10*, 46. [CrossRef]

72. Braga, S.S. Multi-target drugs active against leishmaniasis: A paradigm of drug repurposing. *Eur. J. Med. Chem.* **2019**, *183*, 111660. [CrossRef]

73. Sundar, S.; Olliaro, P.L. Miltefosine in the treatment of leishmaniasis: Clinical evidence for informed clinical risk management. *Ther. Clin. Risk Manag.* **2007**, *3*, 733–740.